Removal of Heavy Metal Ions and Industrial Dyes Using Fe_3O_4-GO-ORMOSIL Ternary Composite

Conrad Lim (3i323), Gavin Lu (3i308), Bezalel Joel Azhar (3i202)

Group 1-17

Abstract

Water pollution is a problem that plagues every country. Common pollutants include heavy metal ions and industrial dyes. Therefore, this study aims to introduce a novel adsorbent for the efficient and rapid removal of heavy metal ions and industrial dyes for water remediation. In this experiment, Zn^{2+} and Fe^{3+} ions as well as Direct Red 80, Methylene Blue and Methyl Orange industrial dyes. These pollutants are widely used in manufacturing industries, and dyes in textile industry especially. Leftover chemicals are disposed of in water bodies, contaminating them which poses several health threats such as risk of dermatitis and cyanosis and long-lasting effects on the environment and aquatic life. The study mainly consists of five stages. Firstly, Fe_3O_4-GO was synthesised. Tetraethoxysilane-vinyltrimethoxysilane mixture was added to a portion of the composite to synthesise Fe_3O_4-GO-ORMOSIL ternary composite. Then, adsorption tests for Fe^{3+}, Zn^{2+}, Methylene Blue, Direct Red 80 and Methyl Orange were conducted for the Fe_3O_4, Fe_3O_4-GO and Fe_3O_4-GO-ORMOSIL. The adsorbency of the composites were recorded and compared. The synthesised composite was found to have adsorbed the highest percentage of every pollutant and had the highest adsorption capacity.

Introduction

Water pollution threatens human, animal and plant life. Anthropogenic activities have caused heavy metals and industrial dyes to be introduced in large quantities in water bodies. (Vhahangwele & Khathutshelo, 2018). With the advent of man-made practices that result in environmental degradation and pollution, the need for environmental remediation has

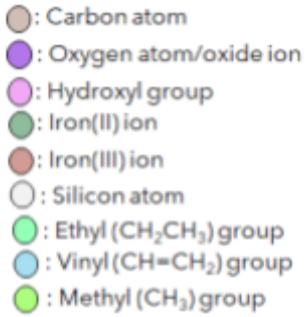

Figure 1.1: Legend for diagrams in Figure 1.2-1.6

reached an all-time high, and with it a rise in research into novel combatants against pollution. The synthesis of graphene oxide, iron oxide and silica nanomaterials has thus been heavily invested in as efficient means for rapid removal of heavy metal ions and industrial dyes which contaminate the environment.

Graphene consists of a two-dimensional atomic layer of sp^2-hybridised carbon atoms lending it a high water permeance (Meng & Baoxia, 2013). The hexagonal structure of atoms grants it a large theoretical specific surface area of $2630 m^2 g^{-1}$ (Xiaolu et al., 2006; Yanwu et al., 2010). The abundance of oxygen-based functional groups allows for surface functionalisation, lending it a hydrophilic nature, better solubility and dispersibility in water and better recyclability (Andrew et al., 2019). Coupled with its excellent chemical stability and associated band structure, graphene oxide is an attractive adsorbent candidate for pollution treatment (Imtithal, Ahmand & Hanafy, 2014).

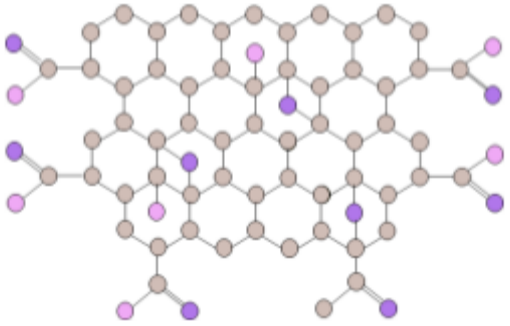

Figure 1.2: Structure of graphene oxide

On the other hand, magnetite facilitates the adsorption of anions and cations effectively from aqueous solutions by binding them to the metal oxide surface (Sharf & Saif, 2017). The high density and small volume of magnetite nanoparticles grant it a high surface area-to-volume ratio and specific surface area of $43.5 m^2 g^{-1}$ (Fawzia et al., 2020). Moreover, the superparamagnetic nature of magnetite nanoparticles and large saturation magnetisation of $82.1 emug^{-1}$ constitutes good regenerability paramount in using the material in a cyclic manner (Min-Rui et al., 2011; Pragnesh & Lakhan, 2014).

Figure 1.3: Structure of magnetite

Organically modified silica (ORMOSIL) is a group of unique materials originating from chemical modification of silica gels via the use of organic precursors (Tushar, Sonia, Avishek, Parameswar &

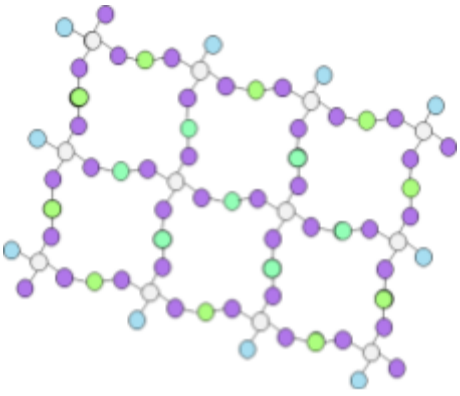

Figure 1.4: Structure of ORMOSIL

Mohammad, 2017). ORMOSIL is perfect for encapsulating inorganic and organic substrates owing to their tunable mechanical properties, high durability and good chemical stability. (Joey, Jonathan, Adi, Lawrence & Alptekin, 2018). As a organic-inorganic hybrid polymer, organic dyes can interact with inorganic groups in ORMOSIL and bind to surface sites (John & Eric, 1998). Coupled with the extensive silica network with oxygen-based functional groups granting ORMOSIL a large pore size and specific surface area, ORMOSIL is a viable adsorbent by itself (Babak, Chil-Hung & Jiangning, 2014).

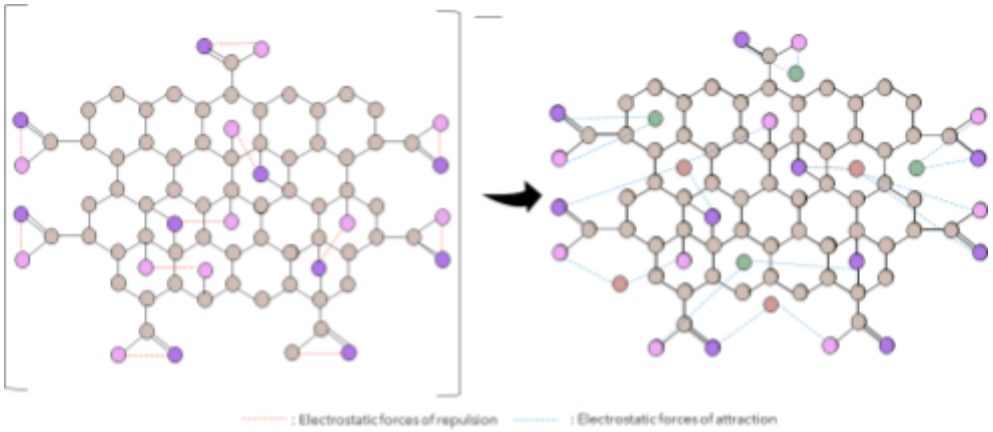

Figure 1.5: Structure of Fe_3O_4-GO

It was also found that Fe_3O_4 and GO work well in combination. On hydration, GO sheets become negatively charged and should disintegrate due to electronic repulsion. However, electrostatic forces of attraction are present due to cross-linked cations in Fe_3O_4, increasing the stability of GO films in water (Che-Ning, Kaylan, Jiaojing, Quan-Hong, Jiajing, 2015). Moreover, the interlayer spacing of GO can swell up to 17.63 Å, leading to poor salt rejection by the GO membranes. It was found that GO membrane can maintain a lower interlayer distance through physical confinement of the GO nanosheets by encapsulating them, maintaining an interlayer spacing of 6.4-9.8 Å. As a result of this controlled spacing, the water permeance is higher and more salts are able to be adsorbed. Hence ORMOSIL also complemented the composite.

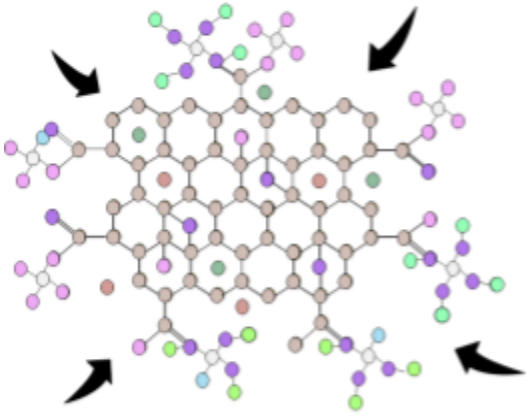

Figure 1.6: Structure of Fe_3O_4-GO-ORMOSIL

Compared to other treatment technologies targeted towards the removal of heavy metal ions and industrial dyes, which include complicated equipment, skilled usage, heavy economic burden, large amounts of byproducts and poisonous intermediates, lower efficiency and higher particularity for groups of pollutants, adsorption technology does not put a toll on finances, is simple in operation and safe to handle (Akba et al., 2017; Sharf & Saif, 2017). This study investigates a novel method of adsorption that leverages on the intrinsic merits of organically modified silica (ORMOSIL).

Objectives and Hypotheses

This study aims to:

1. To synthesise Fe_3O_4-GO-ORMOSIL ternary composite.
2. To investigate the effectiveness of the synthesised Fe_3O_4-GO-ORMOSIL ternary composite in adsorbing zinc and iron(III) ions, as well as direct red 80, methyl orange and methylene blue dyes.

This study hypotheses that:

1. The Fe_3O_4-GO-ORMOSIL ternary composite can be successfully synthesised.
2. The Fe_3O_4-GO-ORMOSIL ternary composite will have an adsorption efficiency greater than that of commercially available rGO.
3. The Fe_3O_4-GO-ORMOSIL ternary composite can be recycled for further use with little reduction to its adsorption efficiency.

Materials and Methods

3.1 Materials

A Hach Company DR/890 Colorimeter was used for measuring the concentration of heavy metal ions. For ultraviolet–visible spectroscopy, a Shimadzu UV-1800 UV spectrophotometer was used.

Tetraethylorthosilicate(TEOS), Vinyltrimethoxysilane(VTMOS), graphene oxide(GO), direct red 80 and methyl orange were purchased from Sigma-Aldrich. Methylene blue was purchased from Unichem. Iron(II) sulfate heptahydrate, iron(iii) chloride hexahydrate, iron(iii) nitrate nonahydrate, zinc sulfate heptahydrate, 25% aqueous ammonia and 1M sodium hydroxide were purchased from GCE Chemicals.

3.2.1 Preparation of pollutants

To prepare 20ppm Zn^{2+} stock solution, 0.0879g of zinc sulfate heptahydrate was dissolved in deionised water in a 1 litre volumetric flask.

To prepare 20ppm Fe^{3+} stock solution, 0.0145g of iron(iii) nitrate nonahydrate was dissolved in deionised water in a 1 litre volumetric flask.

To prepare 20ppm dye stock solutions, 0.020g of the respective dye (methylene blue, direct red 80 and methyl orange) was dissolved in deionised water in a 1 litre volumetric flask.

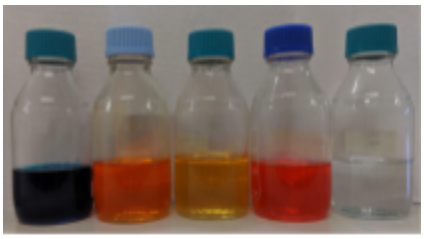

Figure 1: Prepared 20ppm stock solutions

3.2.2 Synthesis of Fe_3O_4

2.57g of iron(II) sulfate heptahydrate and 5.00g of iron(iii) chloride hexahydrate were dissolved in deionised water to give 130ml of a solution with Fe^{2+} and Fe^{3+} ions in a 1:2 molar ratio. 25% aqueous ammonia was then added to maintain the mixture at pH 10 for 1h. The resulting suspension was vacuum filtered, washed to pH 7 and dried in a 60℃ oven for 12h. The composite was collected.

3.2.3 Synthesis of Fe_3O_4 - GO composite

2.00g of graphene oxide was dispersed in 130ml of water. 2.57g of iron(II) sulfate heptahydrate and 5.00g of iron(iii) chloride hexahydrate were dissolved in deionised water to give 130ml of a solution with Fe^{2+} and Fe^{3+} ions in a 1:2 molar ratio. This solution was gradually added to the graphene oxide suspension. 25% aqueous ammonia was then added to maintain the mixture at pH 10 for 1h. The resulting suspension was vacuum filtered, washed to pH 7 and dried in a 60℃ oven for 12h. The composite was collected.

Figure 2:
$FeCl_3 \cdot 6H_2O$-$FeSO_4 \cdot 7H_2O$-GO mixture

3.2.4 Synthesis of Fe3O4 - GO - ORMOSIL ternary composite

5.64ml of tetraethylorthosilicate (TEOS) was added to 3.78ml of vinyltrimethoxysilane (VTMOS) in a 1:1 molar ratio to form 9.00g of TEOS-VTMOS mixture and stirred for 5h for hydrolysis. 1.00 g of Fe_3O_4 - GO (10% specific weight percentage) was then added to the mixture, and the resulting mixture (Figure 3) was shaken at 150rpm for 1h. Then, sodium hydroxide was added to adjust the pH to 14 for base hydrolysis. The reaction mixture was kept in a 60℃ oven for 24h. The resulting suspension was vacuum filtered, washed to pH 7 and dried in a 60℃ oven for 12h. The composite was collected (Figure 4).

Figure 3:
TEOS-VTMOS-Fe_3O_4-GO mixture

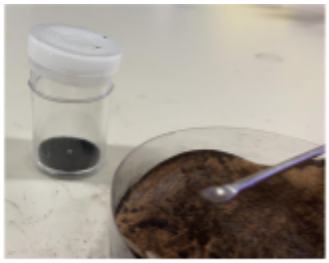

Figure 4: The composite was filtered, dried and collected.

3.2.5 Adsorption tests

50mg of each adsorbent was added to 50ml of 20ppm solution for each pollutant, with a contact time of 12h with constant shaking at 150rpm. 5 replicates were done for each pollutant for Fe_3O_4, Fe_3O_4-GO and Fe_3O_4-GO-ORMOSIL for a total of 75 tests.

Figure 5: Test mixtures shaken at 150rpm for 12h

3.2.6 Recording of results

A magnet was held at the side of the container to attract the magnetic adsorbent before decanting the solution. The final concentration of Zn^{2+} and Fe^{3+} ions were measured with the use of a Hach Company DR/890 Colorimeter. The final concentration of methylene blue, direct red 80 and methyl orange were determined via a calibration curve (Figure 7) correlating absorption in the UV-vis spectrophotometer with the concentration.

Figure 6: Magnetic attraction of adsorbent for separation

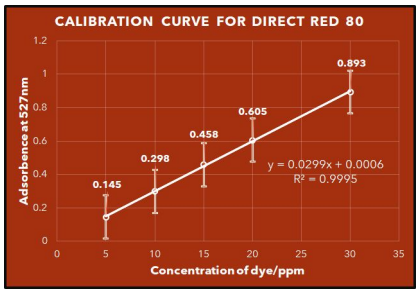

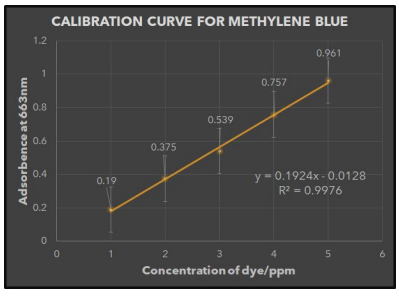

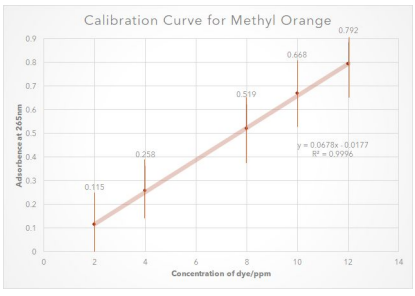

Figure 7.1: Calibration curve for Direct Red 80

Figure 7.2: Calibration curve for Methylene Blue

Figure 7.3: Calibration curve for Methyl Orange

Results and Discussion

FTIR

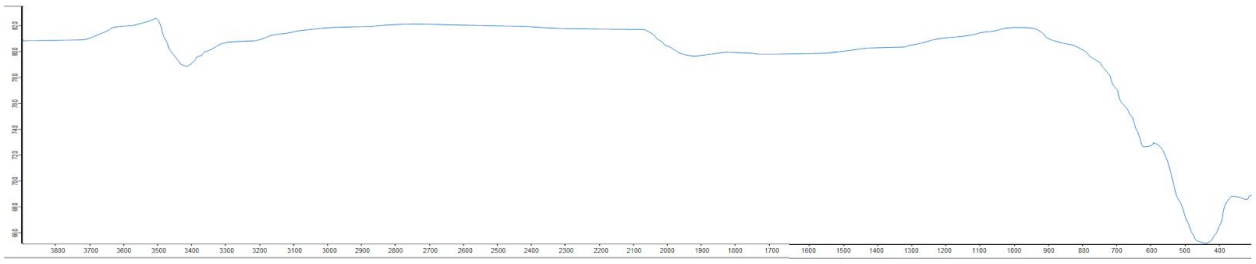

Figure 8.1: FTIR spectrum graph for the synthesised Fe_3O_4

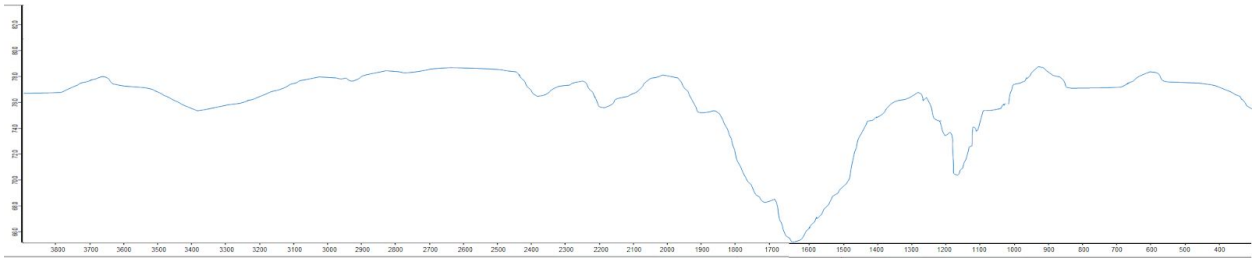

Figure 8.2: FTIR spectrum graph for the synthesised Fe_3O_4-GO-ORMOSIL ternary composite

The Fourier-transform infrared spectroscopy (FTIR) spectra of Fe_3O_4 in Figure 8.1 shows the identification of various absorption bands. The peak at 3400cm^{-1} is characteristic of stretching vibrations of hydroxyl groups. The various peaks at 620cm^{-1} and 480cm^{-1} represent the adsorption band of FeO. With the results obtained from this FTIR similar to the expected FTIR of Fe_3O_4, this study has successfully synthesised Fe_3O_4.

In Figure 8.2, the peak at 3450cm^{-1} is characteristic of the stretching vibrations of silanol (Si-OH) groups. The peak at 1600cm^{-1} represents the stretching vibration of C=C groups. The peak at 1150cm^{-1} is reflective of the stretching and deformation of Si-O-Fe groups. The peak at 550cm^{-1} represents the adsorption band of FeO.

Adsorption Test

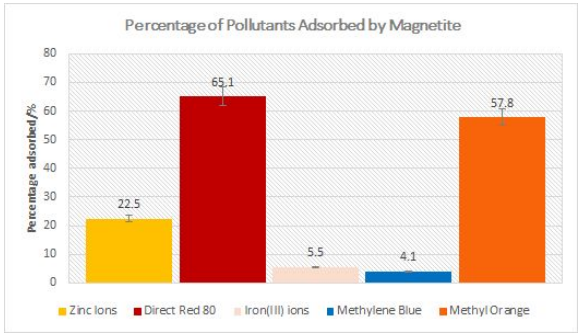

Figure 9.1: Bar graph showing percentage of pollutants adsorbed by Fe_3O_4

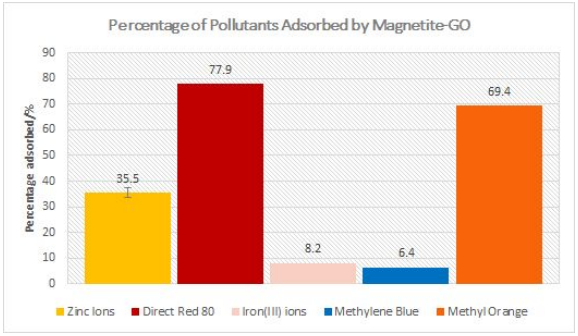

Figure 9.2: Bar graph showing percentage of pollutants adsorbed by Fe_3O_4-GO

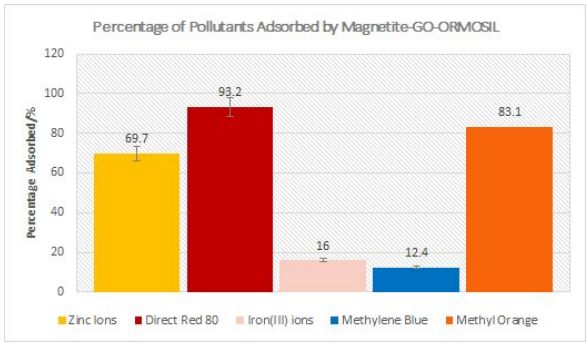

Figure 9.3: Bar graph showing percentage of pollutants adsorbed by Fe_3O_4-GO-ORMOSIL

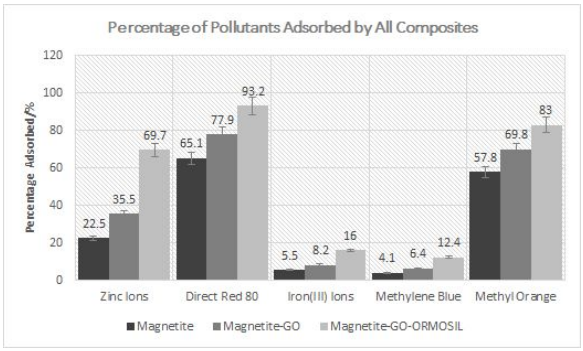

Figure 9.4: Bar graph comparing percentage of pollutants adsorbed by the three composites

In Figure 9.4, direct red 80 was found to be the pollutant that was most adsorbed (65.1%, 77.9%, 93.2%), with a 20.0% increase in adsorption when using the ternary composite compared to the binary composite. Methyl orange was the second most adsorbed (57.8%, 69.8%, 83.1%), with a 19.0% increase in adsorption when using the ternary composite compared to the binary composite, followed by Zn^{2+} (22.5%, 35.5%, 69.7%) with a 96.3% increase in adsorption when using the ternary composite compared to the binary composite, Fe^{3+} (5.5%, 8.2%, 16.0%) with a 95.1% increase in adsorption when using the ternary composite compared to the binary

composite and methylene blue (4.1%, 6.4%, 12.4%) with a 93.7% increase in adsorption when using the ternary composite compared to the binary composite.

Mann Whitney U Test

p-value														
Zn^{2+}			DR80			Fe^{3+}			MB			MO		
U vs B	U vs T	B vs T	U vs B	U vs T	B vs T	U vs B	U vs T	B vs T	U vs B	U vs T	B vs T	U vs B	U vs T	B vs T
0.022	0.012	0.012	0.012	0.012	0.012	0.012	0.012	0.012	0.012	0.012	0.012	0.012	0.012	0.012

Figure 10: Table showing p-values of Mann Whitney U Test, where U (Unary) represents Fe_3O_4, B (Binary) represents Fe_3O_4-GO and T (Ternary) represents Fe_3O_4-GO-ORMOSIL

In Figure 10, the p-value was found to be ranging from 0.012 to 0.022, well below 0.05, hence the results are statistically significant and the null hypothesis can be rejected.

Adsorption Capacity

Adsorption Capacity/mgg^{-1}														
Zn^{2+}			DR80			Fe^{3+}			MB			MO		
U	B	T	U	B	T	U	B	T	U	B	T	U	B	T
4.50	7.10	13.9	13.0	15.6	18.6	1.10	1.64	3.20	0.824	1.29	2.48	11.6	13.9	16.6

Figure 11: Table showing adsorption capacity of composites, where U (Unary) represents Fe_3O_4, B (Binary) represents Fe_3O_4-GO and T (Ternary) represents Fe_3O_4-GO-ORMOSIL

In Figure 11, adsorption capacity of the ternary composite was the highest for every pollutant. A significant increase in adsorption capacity was also observed in Zn^{2+}, Direct Red 80, and Methyl Orange.

Conclusion

The ternary composite was found to have the highest adsorbency for every pollutant. Future experiments could be done to investigate the percentage of pollutants adsorbed as time passes, to

find the time where the composite reaches maximum adsorption capacity as well as investigate the adsorption capacity of the ternary composite for other pollutants. Furthermore, experiments could be done to determine the effect of the specific weight percentage of Fe_3O_4-GO used to form the ternary composite on the adsorption capacity of the ternary composite, as well as the regeneration of the ternary composite. More tests should also be conducted on other heavy metal ions and dyes.

References

Abbas, S. S., Rees, G. J., Kelly, N. L., Dancer, C. E. J., Hanna, J. V., McNally, T. (2018). Facile silane functionalization of graphene oxide. *Nanoscale*, *10*(34), 16231-16242. Retrieved June 14, 2020 from https://doi.org/10.1039/C8NR04781B

Benson, J. J., Sakkos, J. K., Radian, A., Wackett, L. P., Aksan, A. (2018). Enhanced biodegradation of atrazine by bacteria encapsulated in organically modified silica gels. *Journal of Colloid and Interface Science*, *510*, 57-68. Retrieved March 7, 2020 from https://doi.org/10.1016/j.jcis.2017.09.044

Dave, P. N., Chopda, L.V. (2014). Application of Iron Oxide Nanomaterials for the Removal of Heavy Metals. *Journal of Nanotechnology*, *2014*(398569), 1-14. Retrieved February 16, 2020 from https://doi.org/10.1155/2014/398569

El-Dib, F. I., Mohamed, D. E., El-Shamy, O. A. A., Mishrif, M. R. (2020). Study the adsorption properties of magnetite nanoparticles in the presence of different synthesized surfactants for heavy metal ions removal. *Egyptian Journal of Petroleum*, *29*(1), 1-7. Retrieved June 17, 2020 from https://doi.org/10.1016/j.ejpe.2019.08.004

Elsagh, A., Moradi, O., Fakhri, A., Najafi, F., Alizadeh, R., Haddadii, V. (2017). Evaluation of the potential cationic dye removal using adsorption by graphene and carbon nanotubes as adsorbents surfaces. *Arabian Journal of Chemistry*, *10*(2), S2862-S2869. Retrieved March 7, 2020 from https://doi.org/10.1016/j.arabjc.2013.11.013

Gao, M., Zhang, S., Jiang, J., Zheng, Y., Tao, D., Yu, S. (2011). One-pot synthesis of hierarchical magnetite nanochain assemblies with complex building units and their application for water treatment. *J. Mater. Chem.*, *21*(42), 16888-16892. Retrieved July 20, 2020 from https://doi.org/10.1039/C1JM13517A

Hu, M., Mi, B. (2013). Enabling Graphene Oxide Nanosheets as Water Separation Membranes. *Environ. Sci. Technol.*, *47*(8), 3715– 3723. Retrieved July 4, 2020 from https://doi.org/10.1021/es400571g

Juárez, S., Valdiviezo, H., Mogrovejo, C., Achupallas, V. (2019). Detection of heavy metals in hydric resources through the optical analysis of exposed flora. *Light in Nature VII*, 11099. Retrieved 8 April, 2020 from https://doi.org/10.1117/12.2529857

Lei, Y., Chen, F., Luo, Y., Zhang, L. (2014). Synthesis of three-dimensional graphene oxide foam for the removal of heavy metal ions. *Chemical Physics Letters*, *593*, 122-127. Retrieved March 7, 2020 from https://doi.org/10.1016/j.cplett.2013.12.066

Lenntech [Iron (Fe) and water] (n.d.). Retrieved April 2, 2020 from https://www.lenntech.com/periodic/water/iron/iron-and-water.htm

Lenntech [Zinc (Zn) and water] (n.d.). Retrieved April 2, 2020 from https://www.lenntech.com/periodic/water/zinc/zinc-and-water.htm

Liu, X., Ma, R., Wang, X., Ma, Y., Yang, Y., Zhuang, L., …… Wang, X. (2019). Graphene oxide-based materials for efficient removal of heavy metal ions from aqueous solution: A review. *Environmental Pollution*, *252*(A), 62-73. Retrieved February 23, 2020 from https://doi.org/10.1016/j.envpol.2019.05.050

Mackenzie, J. D. (1994). Structures and properties of Ormosils. *Journal of Sol-Gel Science and Technology*, *2*, 81-86. Retrieved July 17, 2020 from https://doi.org/10.1007/BF00486217

Mackenzie, J. D., Bescher, E., (1998). Structures, Properties and Potential Applications of Ormosils. *Journal of Sol-Gel Science and Technology*, *13*(1), 371-377. Retrieved July 17, 2020 from https://doi.org/10.1023/A:1008600723220

Masindi, V., Muedi, K. L., (2018). Environmental Contamination by Heavy Metals. *Heavy Metal*s, *8*. Retrieved Aug 1, 2020 from https://doi.org/10.5772/intechopen.76082.

PubChem [Methylene blue] (n.d.). Retrieved April 10, 2020 from https://pubchem.ncbi.nlm.nih.gov/compound/Methylene-blue

PubChem [Basic red 46] (n.d.). Retrieved April 10, 2020 from https://pubchem.ncbi.nlm.nih.gov/compound/Basic-red-46

Samiey, B., Cheng, C., Wu, J. (2014). Organic-Inorganic Hybrid Polymers as Adsorbents for Removal of Heavy Metal Ions from Solutions: A Review. *Materials*, *7,* 673-726. https://doi.org/10.3390/ma7020673

Satu, T. K., Arora, S., Banik, A., Iyer, P. K., Qureshi, M. (2017). Efficient and Rapid Removal of Environmental Malignant Arsenic(III) and Industrial Dyes Using Reusable, Recoverable Ternary Iron Oxide - ORMOSIL - Reduced Graphene Oxide Composite. *ACS Sustainable Chemistry & Engineering*, *5*(7), 5912-5921. Retrieved February 16, 2020 from https://doi.org/10.1021/acssuschemeng.7b00632

Sheet, I., Kabani, A., Holail, H. (2014). Removal of Heavy Metals Using Nanostructured Graphite Oxide, Silica Nanoparticles and Silica/ Graphite Oxide Composite. *Energy Procedia*, *50*, 130-138. Retrieved February 23, 2020 from https://doi.org/10.1016/j.egypro.2014.06.016

Siddiqui, S. I., Chaudhry, S. A. (2017). Iron oxide and its modified forms as an adsorbent for arsenic removal: A comprehensive recent advancement. *Process Safety and Environmental Protection*, *111*, 592-626. Retrieved February 16, 2020 from https://doi.org/10.1016/j.psep.2017.08.009

Smith, A. T., LaChance, A. M., Zeng, S., Liu, B., Sun, L. (2019). Synthesis, properties, and applications of graphene oxide/reduced graphene oxide and their nanocomposite. *Nano Materials Science*, *1*(1), 31-47. Retrieved June 30, 2020 from https://doi.org/10.1016/j.nanoms.2019.02.004

Tan, C. H. (2015). Determination of Pb(II), Cu(II) and Ni(II) in Water by Direct Measurement using UV/VIS spectrometer. *Universiti Sains Malaysia*. Retrieved April 5, 2020 from http://eprints.usm.my/32085/1/TAN_CH_UN_HO.pdf

World Health Organisation (1996). Zinc in Drinking-water. *Guidelines for drinking-water quality*, *2*(2), 1-5. Retrieved April 1, 2020 from https://www.who.int/water_sanitation_health/dwq/chemicals/zinc.pdf

Yeh, C., Raidongia, K., Shao, J., Yang, Q., Huang, J. (2015). On the origin of the stability of graphene oxide membranes in water. *Nature Chemistry*, *7,*166–170. Retrieved August 1, 2020 from https://doi.org/10.1038/nchem.2145

Zhu, Y., Murali, S., Cai, W., Li, X., Suk, J. W., Potts, J. R., Ruoff, R.S. (2010). Graphene and Graphene Oxide: Synthesis, Properties, and *Applications. Adv. Mate*r, *22*, 3906–3924. Retrieved August 3, 2020 from https://onlinelibrary.wiley.com/doi/pdf/10.1002/adma.201001068

Zaaba, N. I., Foo, K. L., Hashim, U., Tan, S. J., Liu, W. W., Voon, C. H. (2017). Synthesis of Graphene Oxide using Modified Hummer's Method: Solvent Influence. *Procedia Engineering*, *184*, 469-477. Retrieved April 10, 2020 from https://doi.org/10.1016/j.proeng.2017.04.118